water

MDPI

Article

Local Scour around Tandem Double Piers under an Ice Cover

Liansheng Sang [1], Jun Wang [1,*], Tiejie Cheng [1], Zhixing Hou [1] and Jueyi Sui [2,*]

[1] School of Civil and Hydraulic Engineering, Hefei University of Technology, Hefei 230009, China; 13665513421@163.com (L.S.); hfut_chengtj@126.com (T.C.); houhfut@163.com (Z.H.)
[2] School of Engineering, University of Northern British Columbia, Prince George, BC V2N 4Z9, Canada
* Correspondence: junwanghfut@126.com (J.W.); jueyi.sui@unbc.ca (J.S.); Tel.: +86-137-0551-0008 (J.W.); +1-250-960-6399 (J.S.)

Abstract: Compared to the scour around a single pier, the local scour process around tandem double piers is much more complicated. Based on laboratory experiments in a flume, we conducted the scour process around tandem double piers under an ice-covered flow condition. The results showed that when the pier spacing ratio L/D = 2 (where L = the pier spacing distance, and D = the pier diameter), the rear pier (the downstream one) will intensify the horseshoe vortex process behind the front pier, and the scour depth around the front pier will increase by about 10%. As the pier spacing ratio L/D increases, the scour depth around the front pier will gradually decrease. When the pier spacing ratio L/D = 5, sediment scoured around the front pier begins to deposit between these two piers. To initiate a deposition dune between piers, the pier spacing distance under an ice-covered condition is about 20% more than that under an open flow condition. The results also showed that the existence of the rear pier will lead to an increase in the length of the scour hole but a decrease in the depth of the scour hole around the front pier. The local scour around the front pier interacts with the local scour of the rear pier. The maximum scour depth of the scour hole around the rear pier increases first, then decreases and increases again afterward. When the pier spacing ratio L/D = 9, the scour depth around the rear pier is the least. With an increase in the pier spacing ratio, the influence of the local scour around the front pier on the local scour around the rear pier gradually decreases. When the pier spacing ratio L/D is more than 17, the scour around the front pier has hardly any influence on that around the rear pier. The scour depth around the rear pier is about 90% of that around the front pier.

Keywords: ice cover; local scour depth; tandem double piers; pier spacing distance

Citation: Sang, L.; Wang, J.; Cheng, T.; Hou, Z.; Sui, J. Local Scour around Tandem Double Piers under an Ice Cover. *Water* **2022**, *14*, 1168. https://doi.org/10.3390/w14071168

Academic Editor: Maria Mimikou

Received: 27 February 2022
Accepted: 29 March 2022
Published: 6 April 2022

1. Introduction

The local scour around bridge piers/abutments has always been a concern of researchers and engineers. Accurately predicting the scour depth around bridge piers is important for the safety design of a bridge. To date, many studies regarding the local scour process around bridge piers under open flow conditions have been reported. Aksoy et al. [1] carried out experiments to study the scour around a circular pier. The mechanism of the local scour process has been studied. An empirical formula has been proposed to describe the relationship between the scour depth and flow intensity, water depth, and dimensionless time. Using both uniform and non-uniform sands, Chang et al. [2] conducted experiments to study the local scour around bridge piers, and proposed a model describing the local scour depth over a non-uniform sand bed under a steady flow condition. Kothyari et al. [3] carried out laboratory experiments to study local scour around circular piers under the conditions of both steady and unsteady flows. An empirical formula for calculating the time variation in the scour depth was proposed, and on this basis, the expression for the maximum scour depth was obtained by considering the influence of the inhomogeneity and stratification of sediment and the instability of water flow on the scour depth. Sheppard and Miller [4,5] conducted laboratory experiments to study the local scour around bridge piers under movable bed conditions, and proposed an empirical

formula. Based on the experimental data, Pandey et al. [6] developed a new formula for predicting the maximum scour depth in front of piers. Compared to other formulas, the calculated results using their formula agree well with those of observed value.

Under an open flow condition, some studies on local scour around multiple piers or pile groups have been conducted. The results of an experimental study of local scour around pile groups conducted by Ataie-Ashitani and Beheshti [7] showed that the local scour depth around pile groups sometimes increases twice as much as that around a single pier. Using their experimental data and data of other researchers, the correction coefficient for predicting the maximum local scour depth around pile groups was proposed. Kim et al. [8] carried out numerical simulation of the local scour around both tandem double piers and side-by-side double piers, and pointed out that the maximum scour depth around tandem double piers increases with the pier spacing distance first, then decreases gradually with the pier spacing distance, and finally reaches a stable value. They also claimed that the maximum scour depth around side-by-side double piers decreases with the increase in the pier spacing distance. Wang et al. [9] conducted experiments to study the scour problem around tandem double piers by considering different pier spacing distances, flow velocities, and sediment particle sizes. They claimed that the scour depth around the front pier is nearly the same as that around a single pier. Moreover, depending on the flow velocity, the scoured channel bed around the rear pier can be divided into four different zones: a no scouring zone, a synchronous scouring zone, an excessive scouring zone, and a radial offset area. The relationship between the pier spacing distance and the deviation of the radial offset zone was obtained. Liu et al. [10] also studied the local scour around tandem double piers, and claimed that the presence of the transition zone is related to the sediment transportation process from the deposition dune downstream of the front pier to the scour hole around the rear pier. Formulas for determining the critical velocity and predicting the downstream scour depth have been derived. Khaple et al. [11] pointed out that when the pier spacing ratio L/D ranges from 4 to 8, the maximum scour depth around the rear pier of the tandem double piers decreases with the increase in the pier spacing ratio L/D. When $8 < L/D < 10$, the maximum scour depth around the rear pier increases with the pier spacing ratio, and the maximum scour depth around the rear pier is the smallest when $L/D = 8$. When $10 < L/D < 12$, the maximum scour depth around the rear pier approaches a constant which is about 0.80 to 0.87 times of the maximum scour depth around a single pier.

However, the presence of an ice cover in a river imposes a solid boundary to flow. The velocity profile under an ice-covered flow condition is totally different compared to that under an open channel flow. Under an ice-covered flow condition, the maximum velocity occurs between the channel bed and the bottom of the ice cover and is dependent on the relative roughness of these two boundaries [12,13]. Compared to the open flow condition, the scouring process around bridge piers under an ice cover is much more complicated. Bacula and Dargahi [14] carried out experiments to study the local scour around a bridge pier under an ice-covered flow condition. They claimed that the scour depth under an ice-covered flow condition is much greater than that under an open flow condition. Ackerman et al. [15] pointed out that the maximum scour depth under an ice-covered flow condition increases by about 25% to 35% compared to that under an open flow condition. Based on laboratory experiments, Hains [16] claimed that the presence of ice cover leads to about a 21% increase in the local scour depth around bridge piers compared to that under an open flow condition. Wu et al. [17] investigated the scour around a cylindrical bridge pier under ice-covered flow conditions. Empirical formulas have been proposed to calculate the depth and radius of scour holes around piers under both open flow and ice-covered flow conditions. Using three non-uniform natural sands, Wu et al. [18–21] studied the local scour process around both square and circular abutments under both smooth and rough ice-covered flow conditions. They reported that the maximum scour depth around abutments under an ice-covered flow condition depends mainly on the flow Froude number, $D50/H$, and H/D. An empirical formula was proposed to calculate the maximum scour

depth around abutments. By introducing the densiometric Froude number, the influence of geometric shape on the maximum scour depth around abutment was analyzed. It was concluded that the influence of the shape coefficient on the maximum scour depth under ice-covered flow conditions is less than that under an open flow condition. The maximum scour depth increases with the ice cover roughness. Jafari and Sui [22] studied velocity field and turbulence structure around spur dikes with different angles of orientation under ice-covered flow conditions. They reported that the strongest velocity fluctuation occurs immediately above the scour hole surface and very close to the dike tip. With the increase in the dike angle toward upstream, the scour hole becomes larger. Wang et al. [23] compared the difference between the rate of scour depth under an ice-covered flow condition and that under an open flow condition. Their results show that the rate of the scour depth under an ice-covered flow condition is larger than that under an open flow condition. Namaee and Sui [24–28] investigated the local scour problem around side-by-side bridge piers under both open flow and ice-covered flow conditions. Their results showed that the maximum scour depth around piers increases with the ice cover roughness, densiometric Froude number, and pier size. The maximum scour depth decreases with the decrease in the pier size and the increase in pier spacing distance and the particle size of the armor layer in the scour hole. The results of the numerical model were also compared with those of laboratory experiments, and the feasibility of the sediment transport model was verified using the Meyer-Peter and Muller equation.

In summary, many research works have been carried out to study the local scour process around a single pier, multi-piers, and pile group under open flow conditions. To date, however, only a few studies have been conducted to investigate the local scour process around bridge piers or abutments under ice-covered flow conditions. Regarding the local scour process around multiple piers, to our knowledge, only five research works have been reported [24–28]. However, the setup of piers in their studies is a side-by-side installation. The scouring process around tandem double piers under ice-covered flow conditions have never been investigated. In the present study, laboratory experiments were carried out to study the impacts of flow velocities, water depth, and pier spacing distance on the mechanism of local scour around tandem double piers under an ice-covered flow condition.

2. Experiment Setup and Methodology

2.1. Experimental Setup

Laboratory experiments were conducted in the hydraulic laboratory of Hefei University of Technology. The flume used in this experimental study was 26.68 m long and 0.4 m wide. In total, 22 cross sections (CS) for measurements along the flume with an equal spacing distance of 1.2 m were set up. Water flowed out of the water holding tank located upstream of the flume. A triangle weir downstream of the water holding tank was used to determine the flow rate into the flume with the accuracy of 0.1%. A tailgate located at the end of the flume allowed the water to spill over into a downstream reservoir. The downstream reservoir was equipped with a sediment trap and was connected to the suction pipe of a centrifugal pump. The pumping system circulated the water between the downstream reservoir and the water holding tank located upstream of the flume. In the upstream tank, a multi-layer grid was installed to dissipate water energy and reduce water flow oscillation at the flume entrance. Along the left side flume wall, at each cross section, a set of pressure transducers was installed with the accuracy of 0.1 mm, and water levels along the flume were measured (see Figure 1). Between CS-2 and CS-22, a sand bed with an initial thickness of 10 cm was prepared. The median grain size (d50) of the sand bed material was 0.714 mm and the inhomogeneity coefficient η was 1.61. All experiment runs belonged to clear-water scouring. Styrofoam panels were used to model ice cover. The model pier was installed at CS-16. At CS-16, a transparent ruler was affixed to the flume side walls in order to record data such as the initial scouring depth around the piers. The experiment layout is shown in Figure 1.

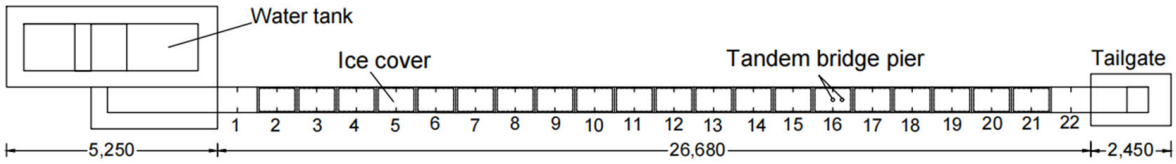

(**a**)

(**b**)

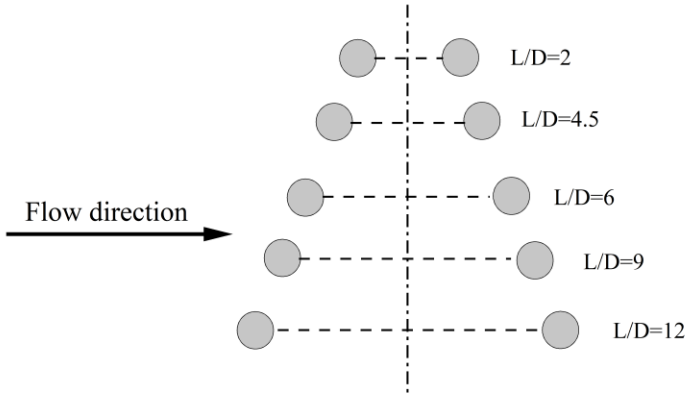

(**c**)

Figure 1. (**a**,**b**) Flume setup for experiments; (**c**) the spacing ratio of tandem double piers (unit: mm).

2.2. Experiment Procedure

The following steps for conducting experiments were strictly followed:

(1) Before each experiment started, the sand bed was leveled, and the slope was maintained at 0 degrees (horizontal) by using a scraping plate. The test pier was installed in the center of the flume at cross section 16.

(2) Afterward, the flume was slowly filled with water to avoid the initial scour of channel bed. When the water level in the flume reached the designated position, the water filling process was finished.

(3) Then, the model ice cover was carefully placed on the water surface. With this step, the preparation for this experiment was completed.

(4) To start each experiment run, a designated discharge through the triangle weir from the water holding tank was kept as a constant. The head (water surface) over the triangular weir was controlled by a point gauge with an accuracy of 0.1 mm. The water level in the flume was maintained at a designated level by adjusting the tailgate at the

downstream end of the flume. Under such a flow condition, this set of experiments was kept running.

(5) At CS-16 where the pier is located, both scour depth and water levels at each cross section were measured once every two minutes during the first half hour, once every five minutes during the 2nd half hour, once every 10 min during the 3rd half hour, and finally, once every 30 min until the end of each experiment run. Experiments showed that after about 6 h, no significant changes in the scouring process and the quasi-equilibrium depth of the scour hole were achieved. However, all experiment runs lasted 16 h to ensure that the local scour process around the tandem double piers reached an equilibrium state. Under such an equilibrium condition, the shape of the deposition dune does not change since the scour process at tandem double piers stops completely, although some sand particles reciprocate inside scour holes but cannot be washed out of scour holes. Then, the model ice cover was removed carefully. By reducing the incoming flow rate from the upstream water holding tank, and increasing the water level by raising the tailgate, the flow velocity in the flume was kept basically at a standstill. Thus, the shape of the scour hole did not change. Then, the bathymetry of the scour hole and deposition dune around the pier was measured by using a point gauge with the accuracy of 0.1 mm. In total, for each survey of the bathymetry of the scour hole and deposition dune, the measurements were conducted at 48 points, including inside the scour hole, along the middle ridge line of the mound, and the outer contour line of the mound. Some variables used in this study are defined and shown in Figure 2.

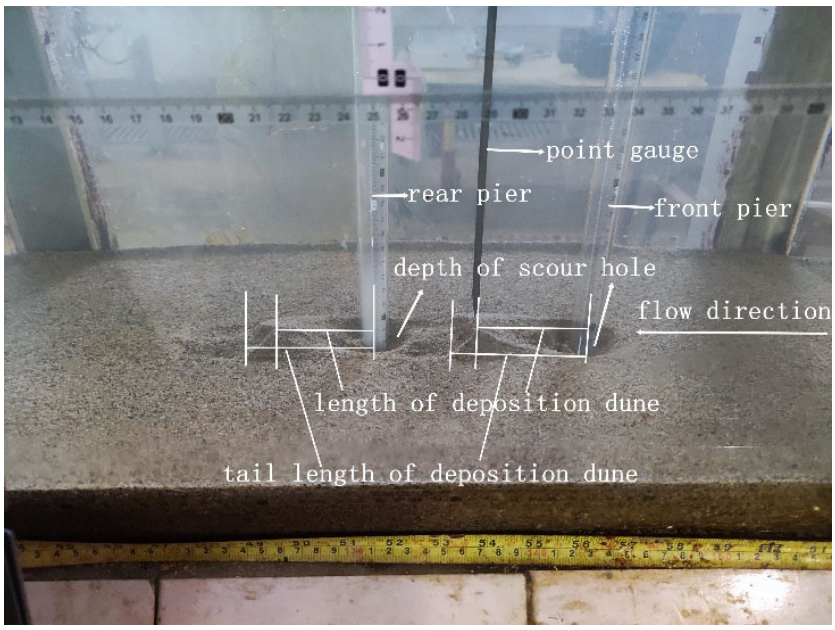

Figure 2. Measurement using a point gauge.

In total, 39 experiments were conducted under different flow conditions (flow depth, velocity) and pier spacing ratios, as shown in Table 1. The flow velocities in this experimental study range from 0.16 to 0.22 m/s.

Table 1. Experimental conditions and results.

Serial Number	V (m/s)	H (m)	D (m)	L (m)	Serial Number	V (m/s)	H (m)	D (m)	L (m)
A1	0.2	0.1	0.02	—	A21	0.2	0.2	0.02	0.09
A2	0.2	0.1	0.02	0.04	A22	0.2	0.2	0.02	0.10
A3	0.2	0.1	0.02	0.09	A23	0.2	0.2	0.02	0.12
A4	0.2	0.1	0.02	0.12	A24	0.2	0.2	0.02	0.17
A5	0.2	0.1	0.02	0.18	A25	0.2	0.2	0.02	0.18
A6	0.2	0.1	0.02	0.22	A26	0.2	0.2	0.02	0.19
A7	0.2	0.1	0.02	0.24	A27	0.2	0.2	0.02	0.24
A8	0.2	0.1	0.02	0.26	A28	0.2	0.2	0.02	0.32
A9	0.2	0.1	0.02	0.32	A29	0.2	0.2	0.02	0.34
A10	0.2	0.1	0.02	—	A30	0.2	0.25	0.02	—
A11	0.2	0.15	0.02	0.04	A31	0.2	025	0.02	0.04
A12	0.2	0.15	0.02	0.09	A32	0.2	0.25	0.02	0.09
A13	0.2	0.15	0.02	0.12	A33	0.2	0.25	0.02	0.12
A14	0.2	0.15	0.02	0.18	A34	0.2	0.25	0.02	0.15
A15	0.2	0.15	0.02	0.24	A35	0.2	0.25	0.02	0.18
A16	0.2	0.2	0.02	—	A36	0.2	0.25	0.02	0.24
A17	0.2	0.2	0.02	0.02	B1	0.16	0.2	0.02	0.18
A18	0.2	0.2	0.02	0.04	B2	0.18	0.2	0.02	0.18
A19	0.2	0.2	0.02	0.05	B3	0.22	0.2	0.02	0.18
A20	0.2	0.2	0.02	0.06	—	—	—	—	—

Note: The flow velocity (V) is the average approaching velocity and division of the discharge by the flow area. The value of H represents the approaching flow.

3. Results and Discussions

3.1. Analysis of Experiment Data

Ample data were collected for these 39 experiments. Table 2 summarizes some measurement results of these experiments. The variation in the depth of the scour hole with time around the front pier of the tandem double piers is compared to that around a single pier case. One can see from Figure 3 that under the same flow condition (approaching flow depth and velocity), the variation in the depth of the scour hole with time around the front pier of the tandem double piers is nearly the same as that around the single pier. When the spacing distance between piers is large enough, the existence of the rear pier hardly affects the local scour around the front pier, and the scour depth around the front pier of tandem double piers is nearly the same as that around a single pier.

As shown in Figure 4, when the pier spacing ratio L/D is less than 5, due to the horseshoe vortex between the front pier and the rear pier, the scoured particles around the front pier are delivered directly into the scour hole around the rear pier and are unable to deposit in the zone between these two piers. Therefore, the scour hole around the front pier is extended to the scour hole around the rear pier to form a large scour hole. With the increase in the pier spacing ratio $L/D > 5$, the effect of the "horseshoe" vortex becomes weak. Consequently, a deposition dune downstream of the front pier begins to develop (between the front pier and rear pier). With a further increase in the pier spacing ratio L/D, both the volume and height of the deposition dune gradually increase. Thus, the interaction between the deposition dune and the rear pier also gradually becomes strong. When the pier spacing ratio $L/D = 9$, the development of the deposition dune between two piers is complete, and the tail of the deposition dune (downstream of the front pier) has a ring shape surrounding the outer edge of the scour hole around the rear pier. When the pier spacing ratio $L/D > 9$, both the shape and size of the deposition dune between two piers hardly change. With a further increase in the pier spacing ratio, the interaction between the deposition dune downstream of the front pier and the local scour around the rear pier gradually becomes weak. When the pier spacing ratio L/D reaches 17, the deposition dune downstream of the front pier has hardly any impact on the local scour around the rear pier, and the local scour process around each of the tandem double piers can be treated as the local scour around a single pier.

Table 2. Experiment results.

Serial Number	Maximum Depth of Scour Hole		Maximum Length of Scour Hole		Maximum Height of Deposition Dune		Maximum Length of Deposition Dune	
	Front Pier	Rear Pier	Front Pier	Rear Pier	Front Pier	Rear Pier	Front Pier	Rear Pier
A1	2.63	—	10.4	—	1.94	—	14.6	—
A2	2.6	1.4	—	—	—	2.06	—	13
A3	2.61	1.6	—	—	—	2.15	—	13.5
A4	2.63	1.7	10	—	1.1	1.46	—	11
A5	2.58	1.54	11.7	—	2.02	1.53	16	12.2
A6	2.6	1.4	11.7	—	2	1.46	14.5	14
A7	2.6	1.5	11.5	—	1.63	1.37	18	14
A8	2.62	1.58	12.3	9.5	1.76	1.37	16.7	13
A9	2.6	2.25	10.4	8.7	1.9	1.74	15	12.7
A10	2.42	—	8.8	—	1.79	—	12.6	—
A11	2.5	1.27	—	—	—	1.73	—	14
A12	2.46	1.48	11	—	—	1.77	—	15
A13	2.4	1.66	10.8	7.1	0.93	1.53	—	16.3
A14	2.37	1.63	9.2	4.6	1.72	1.12	16.2	14.7
A15	2.41	1.7	10.2	8.2	1.71	1.1	14.8	11
A16	2.2	—	9.7	—	1.79	—	12	—
A17	2.43	1.1	—	—	—	1.77	—	11.4
A18	2.22	1.39	—	—	—	1.98	—	11.1
A19	2.22	1.36	—	—	—	2.21	—	10
A20	2.15	1.27	—	—	—	2.33	—	9
A21	2.2	1.52	—	—	—	2.11	—	9.3
A22	2.44	1.17	—	—	—	1.86	—	9.9
A23	2.35	1.26	9.3	6.1	1.32	1.45	8.7	9.7
A24	2.23	1.46	9.6	8.3	1.77	1.37	9.6	10.2
A25	2.2	1.28	9	6.3	1.62	1.04	10	9
A26	2.2	1.42	9.3	6.1	1.83	1.22	9.5	7.5
A27	2.2	1.91	8.9	7.3	1.7	1.39	13	10.3
A28	2.22	2	9.4	8.3	1.9	1.7	11.5	9.5
A29	2.38	0.81	9.1	8.1	1.96	1.78	11.3	9.6
A30	2	—	8.9	—	1.71	—	10.5	—
A31	2.09	0.93	—	—	—	1.75	—	6.7
A32	2.03	1.27	—	—	—	1.76	—	7.7
A33	1.95	1.4	9.4	—	1.38	1.33	8.2	9.1
A34	2	1.3	9.6	6.5	1.58	1.15	10.4	7.5
A35	2.02	1.45	9.3	7.3	1.67	1.16	10.4	7.5
A36	2.03	1.66	8.5	7.6	1.68	1.35	10.9	10.2
B1	0.99	0.87	6.2	6	0.78	0.63	8.1	7.6
B2	1.58	1.27	6.7	6.3	1.43	0.98	7.4	7.3
B3	2.83	1.75	12.3	7.9	1.35	1.65	13.5	18.3

Figure 5 presents the variation in tail length of a deposition dune (L_S) with time (T_i). One can see from Figure 5 that the tail length of a deposition dune around the front pier of tandem double piers is much greater than that for a single pier. This is because that the presence of the rear pier causes changes in the velocity field between the deposition dune downstream of the front pier and the scour hole around the rear pier, and thus, the effect of the "horseshoe" vortex causes more sediment erosion. The tail length of the deposition dune downstream of the rear pier decreases. This is because of the upward flow in front of the front pier and the deposition dune, which results in the decrease in shear stress near the channel bed around the rear pier. Thus, the local scour around the rear pier is weakened, and the tail length of the deposition dune downstream of the rear pier is reduced.

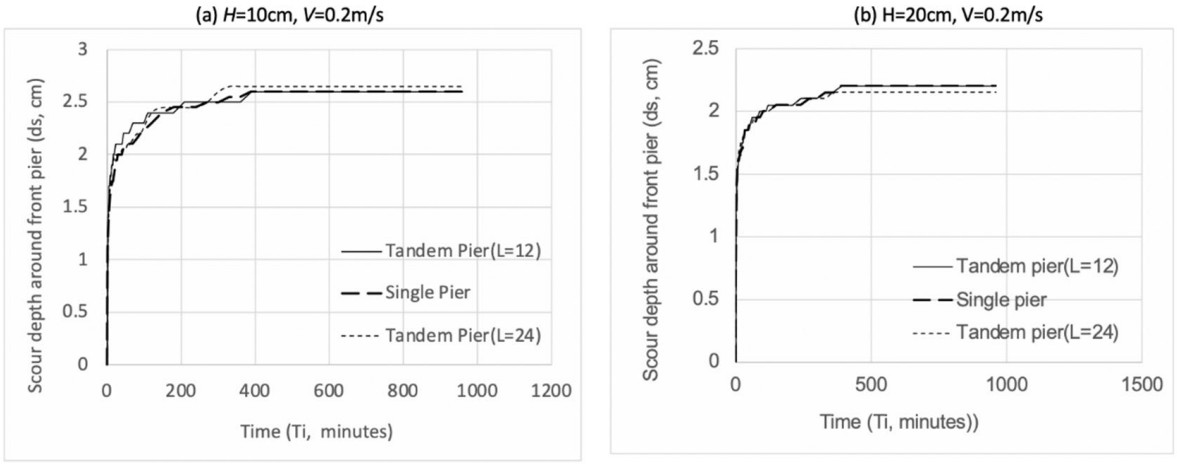

Figure 3. Variation in depth of scour hole with time around the front pier of the tandem double piers compared to that around a single pier condition. (**a**) H = 10 cm, V = 0.2 m/s; (**b**) H = 20 cm, V = 0.2 m/s).

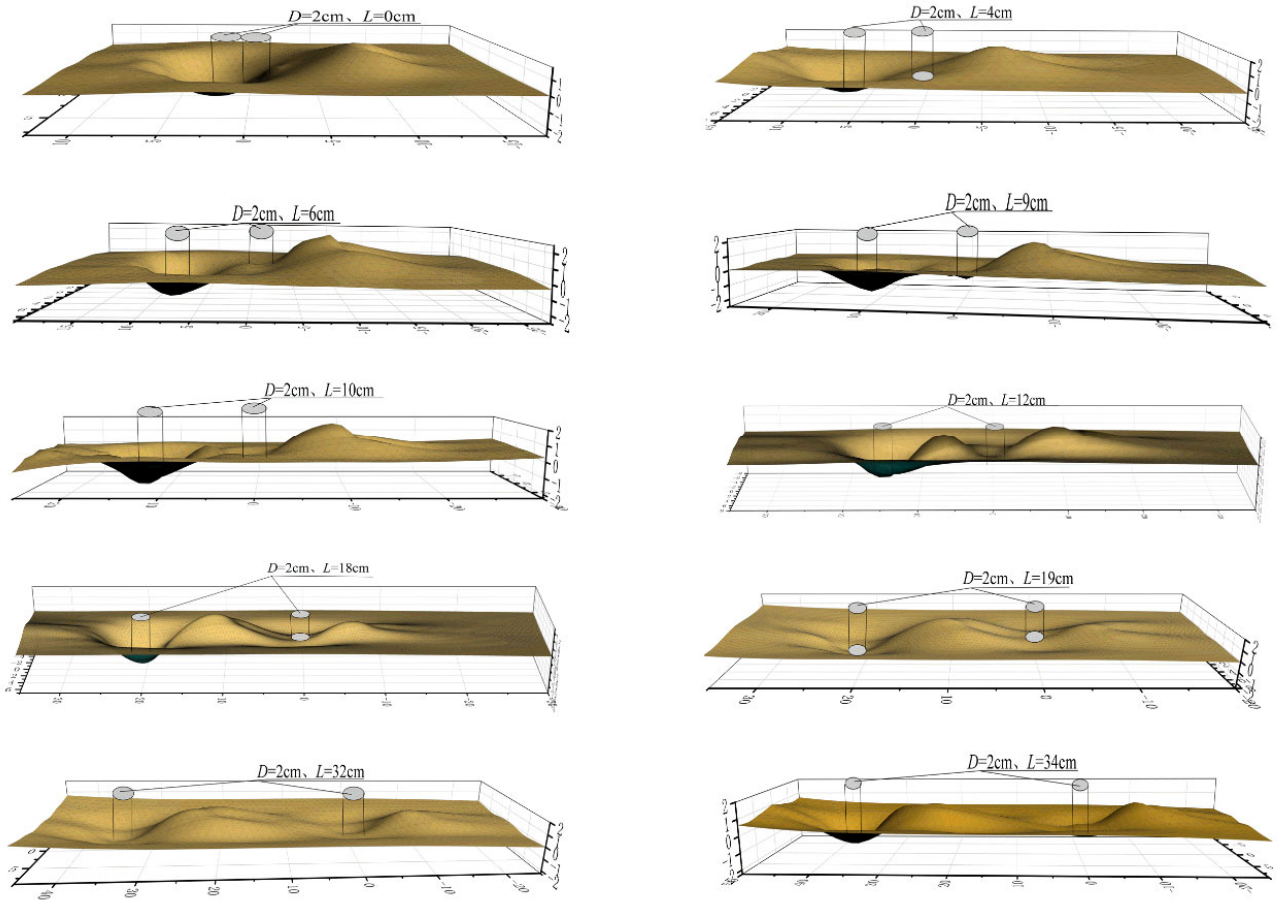

Figure 4. Three-dimensional local scour patterns around tandem double piers for different pier spacing ratio L/D (Note: H = 20 cm, D = 2 cm, and V = 0.2 m/s).

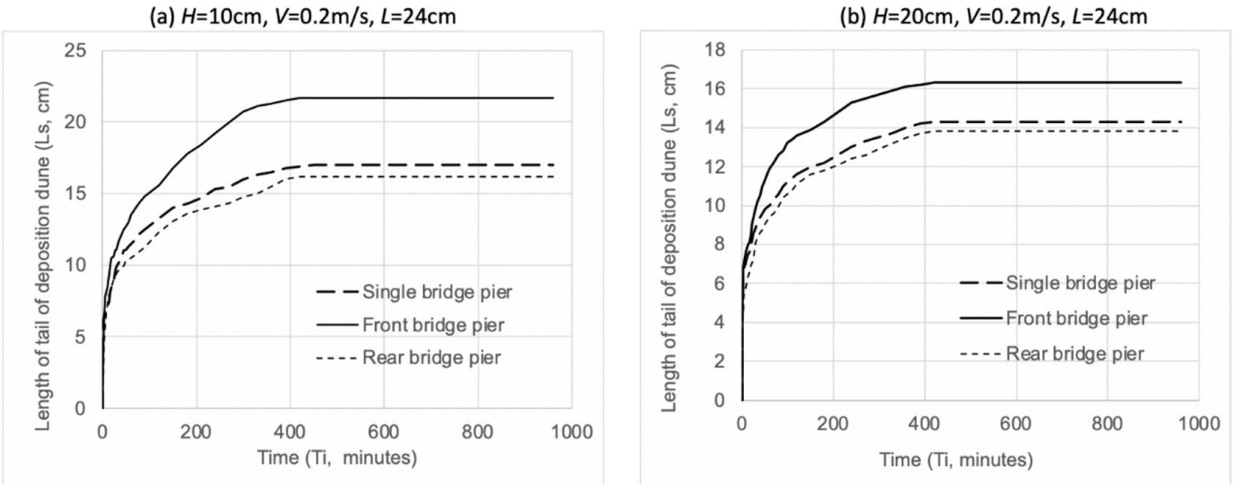

Figure 5. Variation in tail length of deposition dune (L_S) with time (T_i). (**a**) H = 10 cm, V = 0.2 m/s, L = 24 cm; (**b**) H = 20 cm, V = 0.2 m/s, L = 24 cm).

Both the height and length of deposition dunes downstream of tandem double piers have been compared to those of a single pier. As shown in Figure 6, compared to results for the single pier case, in the presence of tandem double piers, the height of the deposition dune downstream of the front pier is lower and its length is longer. This result is consistent with the conclusion from Figure 5. Obviously, the presence of the rear pier should be responsible for this change, since the presence of the rear pier changes the velocity field between the deposition dune in front of the rear pier and the scour hole around the rear pier. Therefore, the transport of sediment particles from the deposition dune became faster, which resulted in a lower but longer deposition dune downstream of the front pier. One can see from Figures 5 and 6 that both the height and length of the tail of the deposition dune downstream of the rear pier are smaller than those of the single pier case. This result reflects the impact of the deposition dune downstream of the front pier. When the spacing distance between piers is small, the deposition dune downstream of the front pier will be scoured and sediment particles will be delivered into the scour hole around the rear pier, which makes the scour process around the rear pier more complicated.

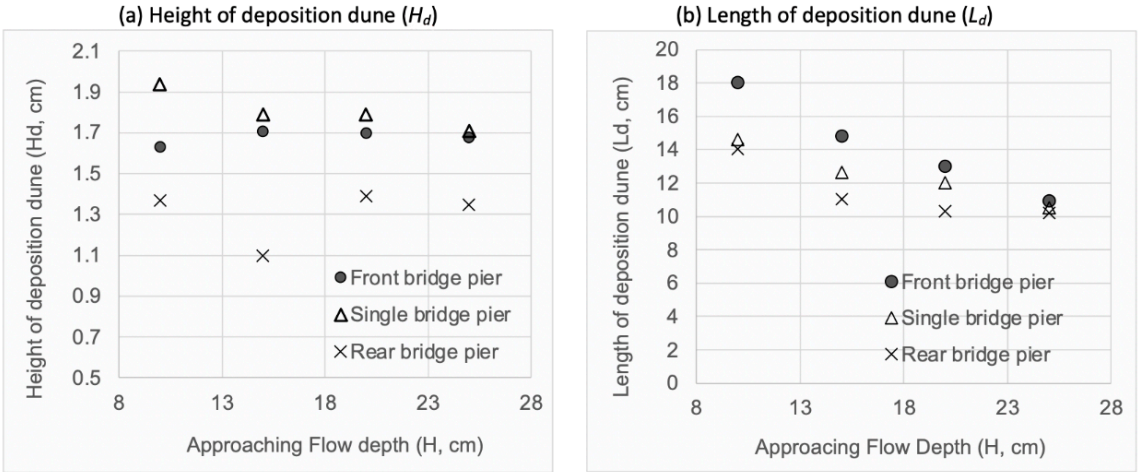

Figure 6. The height and length of deposition dunes downstream of tandem double piers compared to those of a single pier (V = 0.2 m/s, L = 24 cm).

One can see the variations in the length of the deposition dune (Figure 7a), and the variation in the length of the tail of the deposition dune downstream of the rear pier (Figure 7b). The results for the pier spacing distance of L = 12 cm are compared to those for the pier spacing distance of L = 24 cm. The results show that in the presence of tandem double piers, both the length of the deposition dune and the length of the tail of the deposition dune downstream of the rear pier are smaller than those for the single pier case. This is because the deposition dune downstream of the front pier lifts up the flowing current and thus weakens the local scour process around the rear pier. Due to the interaction between the rear pier and the deposition dune downstream of the front pier, the length of the deposition dune downstream of the rear pier for the case of the pier-spacing-distance of 12 cm is smaller than that for L = 24 cm.

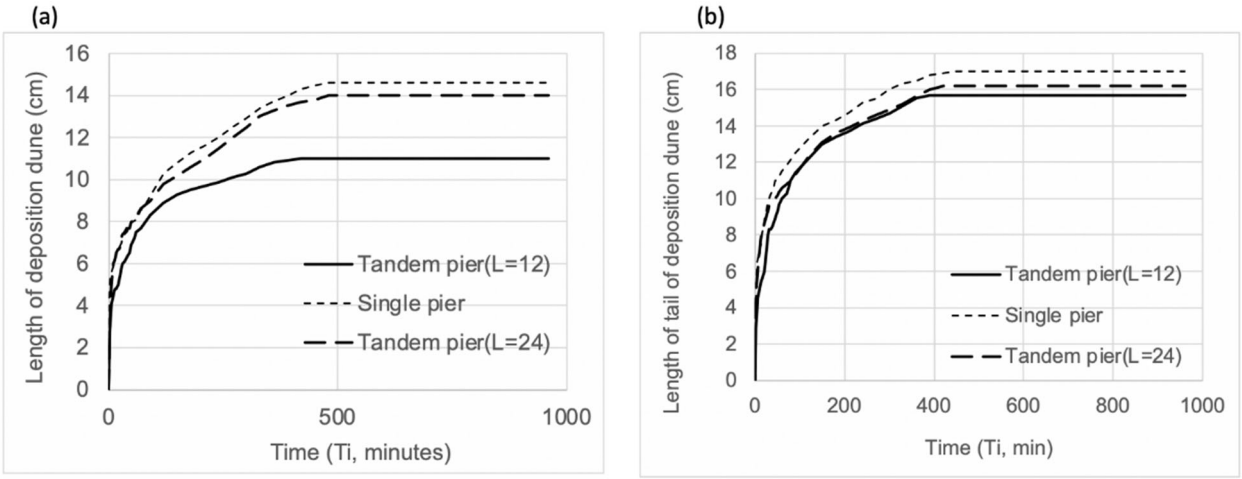

Figure 7. (**a**) Variations in the length of deposition dune downstream of rear pier; (**b**) the length of tail of deposition dune downstream of rear pier. (H = 10 cm, V = 0.2 m/s).

Figure 8 shows the relationship between scour depth and pier spacing ratio. The pier scour contour diagrams for different pier spacing distance are presented in Figure 9. It can be seen from Figure 8 that with the increase in the pier spacing distance (L/D), the dimensionless scour depth (ds/D) around the front pier does not change much and keeps as a constant depending on the flow condition (approaching flow velocity). When the pier spacing distance is L/D = 5, the deposition dune around the front pier begins to initiate between two piers. With the increase in the pier spacing distance, both the volume and height of the deposition dune between two piers gradually increase, and thus, the interaction between the deposition dune and rear piers also gradually increases. From Figures 8b and 9, one can see that when L/D = 9, the tail of the deposition dune downstream of the front pier forms a ring-shaped ridge surrounding the scour hole around the rear piers, and the depth of the scour hole around the rear pier reaches the minimum. At this time, downstream of the deposition dune around the front pier, there exists a ring-shaped deposition dune surrounding the outer edge of the scour hole around the rear pier, and the depth of the scour hole around the rear pier will reach the minimum. When L/D > 9, the shape of the deposition dune between two piers does not changes. With increasing pier spacing distance, the interaction between the deposition dune around the front pier and the local scour around the rear pier gradually weakens. When L/D = 17, there is hardly an interaction between the deposition dune around the front pier and the scour hole around the rear pier; the scouring process around the tandem double piers can be considered as a scour process of two individual single piers. However, due to the presence of an ice cover together with the sediment transport and local scour process, some energy is lost along the flow, including the flows through the scour hole around the front pier, so that the depth of the scour hole around the rear pier is about 90% of that around the front pier.

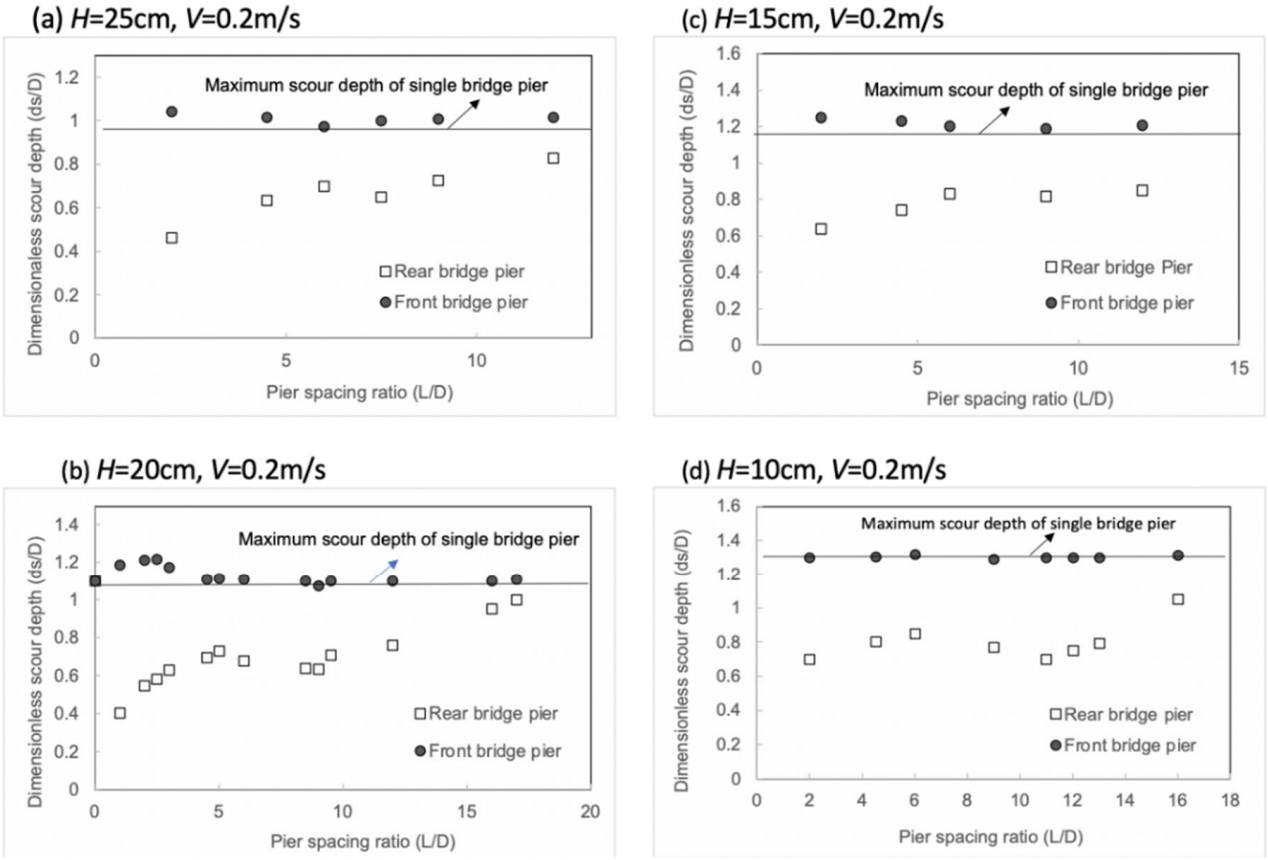

Figure 8. Relationship between scour depth and pier spacing ratio. (**a**) H = 25 cm, V = 0.2 m/s; (**b**) H = 20 cm, V = 0.2 m/s; (**c**) H = 15 cm, V = 0.2 m/s; (**d**) H = 10 cm, V = 0.2 m/s).

3.2. Empirical Expression for Calculating Scour Depth

The dimensionless number $(L_{sp}/D)*(D_{50}/D)^2*\eta$ is used to describe the influence of the pier spacing distance. The relationship between $(L_{sp}/D)*(D_{50}/D)^2*\eta$ and the flow Froude number (F_r) is presented in Figure 10. The data for open flow conditions were obtained from Liu (2018), who conducted experiments using tandem double piers. The results of the analysis show that under an ice-covered flow condition, the presence of the front pier causes a more significant effect with a larger influencing range compared to that under an open flow condition.

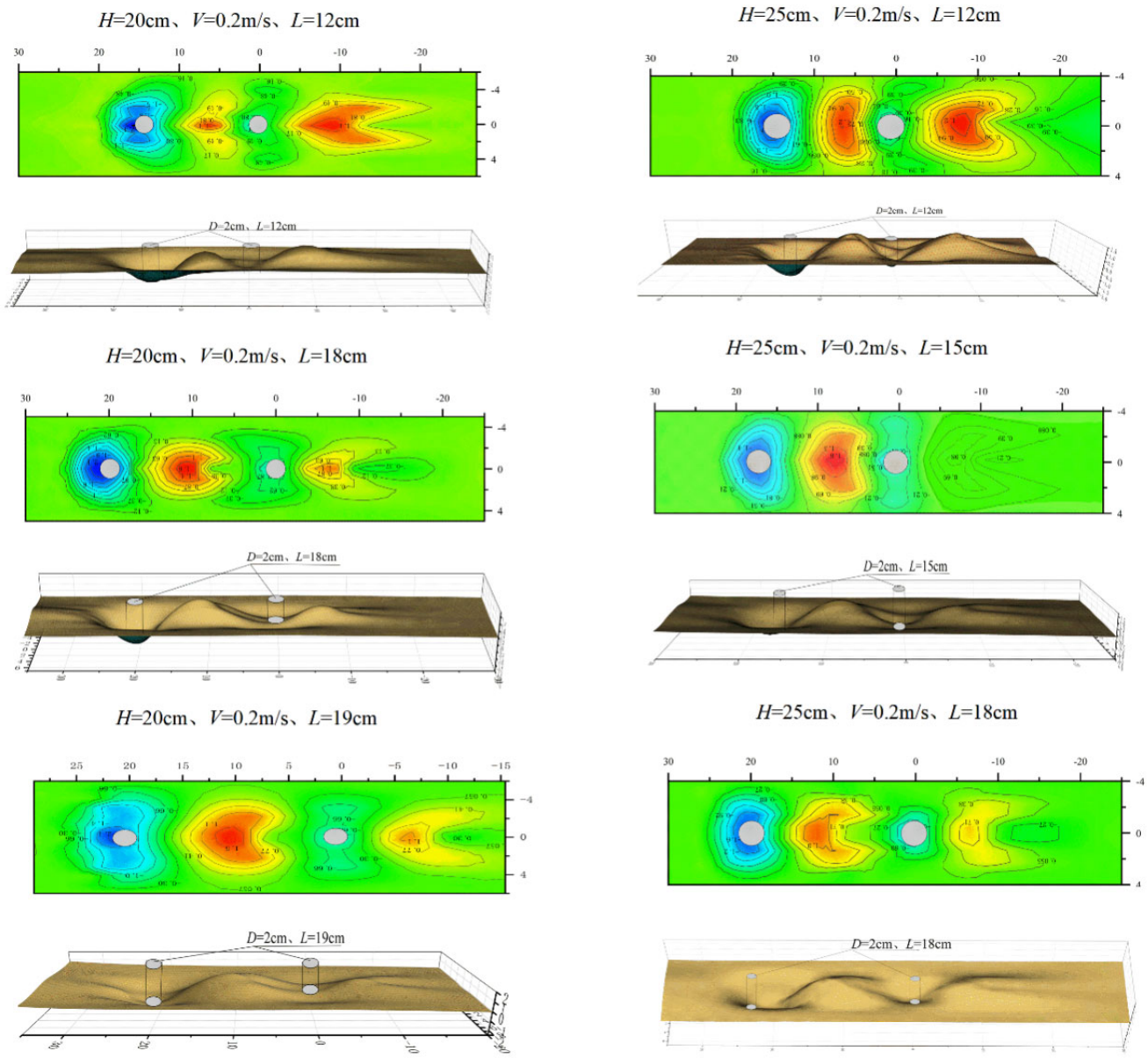

Figure 9. Pier scour contour diagrams for different pier spacing distances.

The depth of a scour hole around a pier is affected by hydraulic conditions, bed material, and the pier spacing distance, as shown in Figure 11. Considering a bridge pier in a river with steady and uniform flow, the following parameters may influence the depth of a scour hole (d_S) around the pier: (1) median grain size of the bed material (D_{50}); (2) flow Froude number (F_r); (3) pier spacing distance (L); (4) pier diameter (D). Thus, the relationship between dimensionless local scour depth under an ice-covered flow condition and factors affecting the depth of the scour hole around a pier can be expressed as follows:

$$\frac{d_s}{D} = kF_r{}^a\left(\frac{L}{D}\right)^b\left(\frac{D_{50}}{H}\right)^c \quad (1)$$

where k, a, b, and c are coefficients.

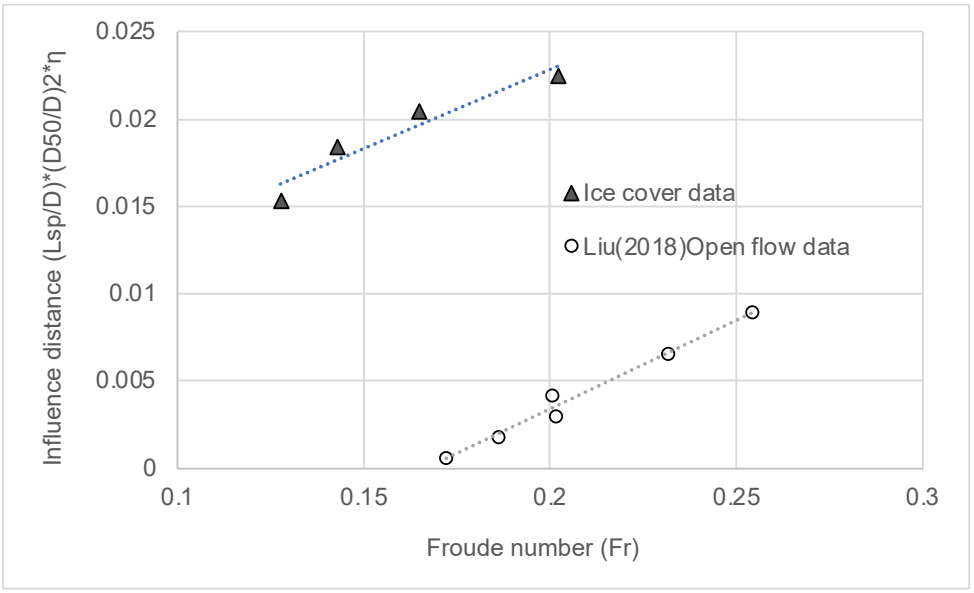

Figure 10. Relationship between the influence distance of the front pier on the rear pier and the flow Froude number.

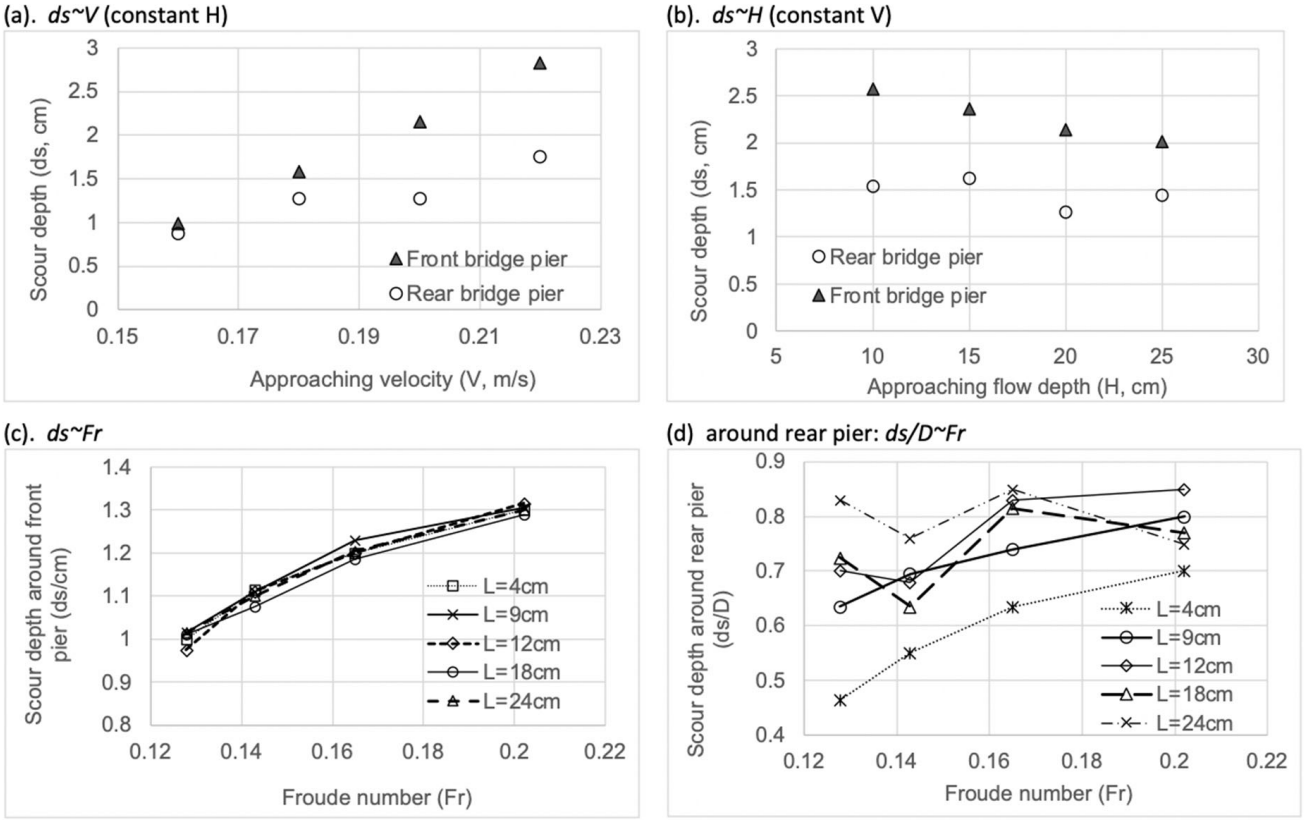

Figure 11. Relationship between scour depth (*ds*, or d_S/D) and hydraulic conditions (*V, H*, or *Fr*).

Based on data collected from laboratory experiments, the following relationships for determining the scour depth around both the front pier and the rear pier under an ice-covered flow condition are obtained, respectively:

Scour depth around the front pier:

$$\frac{d_s}{D} = F_r^{2.462}\left(\frac{L}{D}\right)^{-0.031}\left(\frac{D_{50}}{H}\right)^{-0.858} \quad (2)$$

Scour depth around the rear pier:

$$\frac{d_s}{D} = F_r^{1.462}\left(\frac{L}{D}\right)^{0.189}\left(\frac{D_{50}}{H}\right)^{-0.475} \quad (3)$$

One can see from Equations (2) and (3) that with the increase in the flow Froude number (F_r), the dimensionless depths (d_s/D) of the scour hole around both the front and rear piers increase. The scour depth (d_s/D) around the front pier increases with the decrease in the pier spacing ratio (L/D) between piers. However, the scour depth (d_s/D) around the rear pier increases with the increase in the pier spacing ratio (L/D) between piers. Figure 12 shows the observed scour depths around the front pier and rear pier compared to those calculated using Equations (2) and (3), respectively. One can see that the calculation results agree well with the observations.

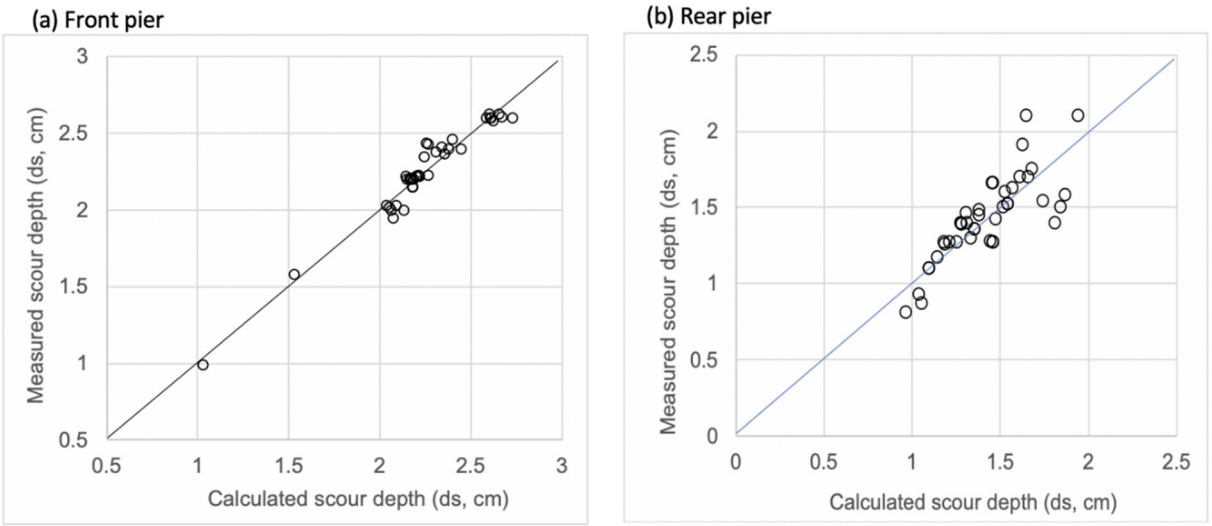

Figure 12. Comparison between calculated scour depths and those of observations. (**a**) Front pier; (**b**) Rear pier.

4. Conclusions

The present experimental study mainly focused on the influence of the pier spacing distance on the depth of scour holes and the height of deposition dunes downstream of piers in ice-covered flow conditions. The results of the present study have been compared to those of the local scour around a single pier under the same conditions. The following conclusions have been drawn from this experimental study:

1. Under an ice-covered flow condition, the patterns of local scour around the tandem double piers depends on the spacing distance between the piers. If the spacing distance between the piers is zero, the local scour process around the tandem double piers should be treated as a single pier scour. With the increase in the spacing distance between piers, the scour depth around the front pier under an ice-covered flow condition increases by about 10% compared to that under a single pier case. Moreover, with the increase in the pier spacing ratio, the scour depth around the front pier will gradually decrease. When the pier spacing ratio L/D = 5, sediment scoured at the front

pier begins to deposit between these two piers. To initiate a deposition dune between piers, the pier spacing distance under an ice-covered condition is about 20% more than that under an open flow condition. The existence of the rear pier will increase the length of the scour hole but reduce the depth of the scour hole around the front pier. The maximum scour depth around the rear pier increases first, then decreases and increases again afterward. When the pier spacing ratio L/D = 9, the local scour depth around the rear pier is the least. With the increase in the pier spacing ratio, the influence of the local scour around the front pier on the local scour around the rear pier gradually decreases. When the pier spacing ratio L/D is more than 17, the local scour around the front pier has hardly any influence on that around the rear pier. The scour depth around the rear pier is about 90% of that around the front pier.

2. Under the same experimental conditions, compared with the results of local scour around a single pier, when the pier spacing ratio $L/D > 4.5$, the height of the deposition dune downstream of the front pier is lower, but the length of the deposition dune downstream of the front pier is longer. Both the height and length of the deposition dune downstream of the rear pier are smaller than those of the single pier case.
3. Relationships for calculating the scour depth around both the front pier and rear pier under ice-covered flow conditions were obtained. With the increase in the flow Froude number (F_r), the depths (d_s/D) of the scour hole around both the front and rear piers increase. The scour depth (d_s/D) around the front pier increases with the decrease in the pier spacing ratio (L/D) between piers. However, the scour depth (d_s/D) around the rear pier increases with the increase in the pier spacing ratio (L/D) between piers. The calculation results using proposed equations agree well with those of observations.

Author Contributions: L.S.: Laboratory works, data curation, formal analysis, methodology, and writing—original draft preparation; J.W.: Conceptualization, laboratory supervision, methodology, funding acquisition, writing—original draft preparation; T.C.: Laboratory works, data curation, investigation; Z.H.: Laboratory works, data curation, investigation; J.S.: Conceptualization, formal analysis, methodology, writing—review and editing. All authors have read and agreed to the published version of the manuscript.

Funding: This research was supported by the National Natural Science Foundation of China (grant nos. 51879065). The authors are grateful for the financial support.

Institutional Review Board Statement: Not applicable.

Informed Consent Statement: Not applicable.

Data Availability Statement: The data are available in the case that it is required.

Conflicts of Interest: The authors declare no conflict of interest.

References

1. Aksoy, A.O.; Bombar, G.; Arkis, T.; Guney, M.S. Study of the time-dependent clear water scour around circular bridge piers. *J. Hydrol. Hydromech.* **2017**, *65*, 26–34. [CrossRef]
2. Chang, W.Y.; Lai, J.S.; Yen, C.L. Evolution of Scour Depth at Circular Bridge Piers. *J. Hydraul. Eng.* **2004**, *130*, 905–913. [CrossRef]
3. Kothyari, U.C.; Garde, R.C.J.; Raju, K.G.R. Temporal variation of scour around circular bridge piers. *J. Hydraul. Eng.* **1992**, *118*, 1091–1106. [CrossRef]
4. Sheppard, D.M.; Odeh, M.; Glasser, T. Large scale clear-water local pier scour experiments. *J. Hydraul. Eng.* **2004**, *130*, 957–963. [CrossRef]
5. Sheppard, D.M.; Miller, W. Live-bed local pier scour experiments. *J. Hydraul. Eng.* **2006**, *132*, 635–642. [CrossRef]
6. Pandey, M.; Sharma, P.K.; Ahmad, Z.; Singh, U.K. Experimental investigation of clear-water temporal scour variation around bridge pier in gravel. *Environ. Fluid Mech.* **2018**, *18*, 871–890. [CrossRef]
7. Ataie-Ashtiani, B.; Beheshti, A.A. Experimental investigation of clear-water local scour at pile groups. *J. Hydraul. Eng.* **2006**, *132*, 1100–1104. [CrossRef]
8. Kim, H.S.; Nabi, M.; Kimura, I.; Shimizu, Y. Numerical investigation of local scour at two adjacent cylinders. *Adv. Water Resour.* **2014**, *70*, 131–147. [CrossRef]

9. Wang, H.; Tang, H.W.; Liu, Q.S.; Wang, Y. Clear-water local scouring around three piers in a tandem arrangement. *J. Hydraul. Eng.* **2016**, *59*, 888–896. [CrossRef]
10. Liu, Q.S.; Tang, H.W.; Wang, H.; Xiao, J.F. Critical velocities for local scour around twin piers in tandem. *J. Hydrodyn.* **2018**, *30*, 1165–1173. [CrossRef]
11. Khaple, S.; Hanmaiahgari, P.R.; Gaudio, R.; Dey, S. Interference of an upstream pier on local scour at downstream piers. *Acta Geophys.* **2017**, *65*, 29–46. [CrossRef]
12. Sui, J.; Faruque, M.A.A.; Balachandar, R. Local scour caused by submerged square jets under ice cover. *ASCE J. Hydraul. Eng.* **2009**, *135*, 316–319. [CrossRef]
13. Sui, J.; Wang, J.; He, Y.; Krol, F. Velocity profiles and incipient motion of frazil particles under ice cover. *Int. J. Sediment Res.* **2010**, *25*, 39–51. [CrossRef]
14. Batuca, D.; Dargahi, B. Some experimental results on local scour around cylindrical piers for open and covered flow. In Proceedings of the 3rd International Symposium on River Sedimentation, Jackson, MS, USA, 31 March–4 April 1986.
15. Ackermann, N.L.; Shen, H.T.; Olsson, P. Local scour around circular piers under ice covers. Ice in the Environment. In Proceedings of the 16th IAHR International Symposium on Ice, Dunedin, New Zealand, 2–6 December 2002.
16. Hains, D.B. An Experimental Study of Ice Effects on Scour at Bridge Piers. Ph.D. Thesis, Lehigh University, Bethlehem, PA, USA, 2004.
17. Wu, P.; Balachandar, R.; Sui, J. Local scour around bridge piers under ice-covered conditions. *J. Hydraul. Eng.* **2016**, *2*, 115–121. [CrossRef]
18. Wu, P.; Hirshfield, F.; Sui, J. Further studies of incipient motion and shear stress on local scour around bridge abutment under ice cover. *Can. J. Civ. Eng.* **2014**, *41*, 892–899. [CrossRef]
19. Wu, P.; Hirshfield, F.; Sui, J.; Wang, J.; Chen, P.P. Impacts of ice cover on local scour around semi-circular bridge abutment. *J. Hydrodyn.* **2014**, *26*, 10–18. [CrossRef]
20. Wu, P.; Hirshfield, F.; Sui, J. Local scour around bridge abutments under ice covered condition-an experimental study. *Int. J. Sediment Res.* **2015**, *30*, 39–47. [CrossRef]
21. Wu, P.; Hirshfield, F.; Sui, J. Armour layer analysis of local scour around bridge abutments under ice cover. *River Res. Appl.* **2015**, *31*, 736–746. [CrossRef]
22. Jafari, R.; Sui, J. Velocity field and turbulence structure around spur dikes with different angles of orientation under ice covered flow conditions. *Water* **2021**, *13*, 1844. [CrossRef]
23. Wang, J.; Li, Z.Q.; Cheng, T.J.; Sui, J. Experimental study on local erosion of piers under ice cover with time. *J. Hydraul. Eng.* **2021**, *52*, 1174–1182.
24. Namaee, M.R.; Sui, J. Impact of armour layer on the depth of scour hole around side-by-side bridge piers under ice-covered flow condition. *J. Hydrol. Hydromech.* **2019**, *67*, 240–251. [CrossRef]
25. Namaee, M.R.; Sui, J. Effects of ice cover on the incipient motion of bed material and shear stress around side-by-side bridge piers. *Cold Reg. Sci. Technol.* **2019**, *165*, 102811. [CrossRef]
26. Namaee, M.R.; Sui, J. Local scour around two side-by-side cylindrical bridge piers under ice-covered condition. *Int. J. Sediment Res.* **2019**, *34*, 355–367. [CrossRef]
27. Namaee, M.R.; Sui, J. Velocity profiles and turbulence intensities around side-by-side bridge piers under ice-covered flow condition. *J. Hydrol. Hydromech.* **2020**, *68*, 70–82. [CrossRef]
28. Namaee, M.R.; Sui, J.; Wu, Y.; Linklater, N. Three-dimensional numerical simulation of local scour around circular side-by-side bridge piers with ice cover. *Can. J. Civ. Eng.* **2021**, *48*, 1335–1353. [CrossRef]